ECS Electrochemistry Letters, **3** (1) A8-A10 (2014)
2162-8726/2014/3(1)/A8/3/$31.00 © The Electrochemical Society

Facile Synthesis of Fe_2O_3 Nanoflakes and Their Electrochemical Properties for Li-Air Batteries

Zhian Zhang,[z] Geng Zhou, Wei Chen, Yanqing Lai,[z] and Jie Li

School of Metallurgy and Environment, Central South University, Changsha, Hunan 410083, China

Fe_2O_3 nanoflakes were synthesized via a hydrothermal method and employed as a cathode catalyst for non-aqueous Li-air batteries. The synthesized Fe_2O_3 nanoflakes with an average diameter of ∼90 nm were well crystallized. The Fe_2O_3 nanoflakes manifest superior catalytic activity for oxygen reduction reaction and evolution reaction in Li-air batteries. The discharge-recharge voltage gap of Fe_2O_3/super P is reduced to ∼0.83 V. By the addition of Fe_2O_3, the cell exhibits a capacity of ∼5200 mAh/$g_{electrode}$, and shows a rate capability of ∼2000 mAh/$g_{electrode}$ at a current density of 0.4 mA/cm^2, and it also has a stable capacity performance after 30 cycles.
 [DOI: 10.1149/2.006401eel]

Manuscript submitted September 3, 2013; revised manuscript received October 17, 2013. Published November 14, 2013.

Li-air (Li-O_2) batteries have attracted worldwide attention in recent years owing to their high theoretical energy density (about 5200 Wh/kg, including O_2), which makes Li–air batteries one of the most promising candidates for the future energy sources.[1–3] Since they were firstly presented by Abraham in 1996,[1] extensive research on Li-air batteries has been conducted.[3–7] However, many challenges are still required to be overcome before they can be considered as a viable alternative for practical applications.[8,9]

One of the biggest challenges that limit the practical use of the Li–air batteries is the critical polarization during the discharge and charge processes.[8] The huge cell polarization may be related to the sluggish kinetics oxygen reduction reaction (ORR) and oxygen evolution reaction (OER) of cathodic materials for Li-air batteries.[10] It is well-known that nanosized catalysts not only play a significant role in both ORR and OER, but also affect the cyclability and rate capacity of Li-air batteries due to the increased active sites.[11] Therefore, the development of a highly efficient and low-cost electrocatalysis to facilitate the ORR/OER is quite vital for Li-air batteries. Transition metal oxides (MnO_2, Co_3O_4, Fe_2O_3 and their composite),[5,11–13] noble metals (Au, Pt),[7,14] and non-precious metals (CoFe/C) have previously been explored as catalysts for Li-air batteries.[15]

Fe-based catalysts can exhibit efficient electrocatalytic activities for the ORR in fuel cells.[16] Li et al. revealed the excellent electrocatalytic activity of Fe_2O_3 for H_2O_2 decomposition.[17] Recently, Zhang et al. have synthesized Fe_2O_3/graphene through an electrochemical deposition method to investigate its catalytic capacity in Li-air batteries,[12] which presented excellent electrochemical properties, but the polarization performance still needs to be improved. These studies inspired us continue to exploit the electrocatalytic performance of Fe_2O_3 for Li-air batteries.

In this research, Fe_2O_3 nanoflakes were synthesized by a simple hydrothermal method and used as a cathode catalyst in non-aqueous Li-air batteries. The Fe_2O_3 nanoflakes show high catalytic properties for both ORR and OER in the batteries.

Experimental

Materials synthesis.— All the chemicals used herein were of analytical purity. In a typical synthesis progress, 0.20 g $FeCl_3 \cdot 6H_2O$ was dissolved in 40 mL of a co-solvents containing glycerol (6 mL) and de-ionized water (34 mL). The mixture was stirred for 30 min and then transferred into a 60 mL Teflon-lined stainless steel autoclave, heated to 160°C in an oven for 10 h. After cooling to room temperature, the red product was collected by centrifugation, and washed with de-ionized water and ethanol for several times, and then dried at 80°C for 24 h.

Materials characterizations.— The synthesized product was analyzed by X-ray powder diffraction (XRD, Rigaku D/max 2500VB/PC, Cu K_α, $\lambda = 1.5406$ Å). The morphology of the sample was characterized with field emission scanning electron microscopy (FESEM, Nova NanoSEM 230) and transmission electron microscopy (TEM-2100F).

Electrochemical tests.— Electrochemical characterizations were carried out in Li-air coin batteries consisting of a Li foil anode, an electrolyte of 1 M LiTFSI in TEGDME, and an air electrode. The air electrodes were prepared by casting a mixture containing 15 wt% Fe_2O_3, 75 wt% super P and 10 wt% PVDF, or 90 wt% super P and 10 wt% PVDF on a Ni foam. The galvanostatic discharge/charge performance of the Li–air battery was observed at a current density of 0.05–0.4 mA/cm^2. It is noted that the specific capacity was calculated based on the total mass of the air electrode. Cyclic voltammograms were recorded in the potential range of 2.0–4.2 V at a scan rate of 0.5 mV/s. The polarization curves were obtained at a scan rate of 2 mV/s.

Results and Discussion

Characterization of Fe_2O_3.— The successful synthesis of Fe_2O_3 was confirmed by X-ray diffraction (XRD), as shown in Fig. 1a. All the marked peaks can be readily indexed to a pure rhombohedral phase of Fe_2O_3 with cell constants: a = 5.036 Å, b = 5.039 Å, c = 13.749 Å, which matches well with the standard patterns of Fe_2O_3 (space group *R3c*, JCPDS: 33–0664). Fig. 1b–1d shows the morphologies of Fe_2O_3 nanoflakes characterized by FESEM, TEM and HRTEM. It can be detected from Fig. 1b that Fe_2O_3 nanoflakes have a diameter of ∼90 nm. TEM image shown in Fig. 1c further confirms that the diameter of the Fe_2O_3 nanoflakes is ∼90 nm. The high resolution TEM image (Fig. 1d) indicates that the nanoflakes are well crystallized. And the measured lattice fringe is consistent with the spacing of the (012) crystal plane of rhombohedral Fe_2O_3.

Electrochemical properties.— The electrocatalytic activity of Fe_2O_3 nanoflakes in Li-air coin batteries was tested. Fig. 2a shows the cyclic voltammograms (CV) for the electrode with Fe_2O_3 nanoflakes in Li–air batteries. Compared with the CV profile of Super P electrode without Fe_2O_3 nanoflakes, the addition of Fe_2O_3 significantly increases the ORR voltage and the ORR current peak. In the anodic scan, the electrode with Fe_2O_3 nanoflakes exhibits two obvious OER peaks, which should be attributed to the oxidation of LiO_2 and Li_2O_2, respectively.[18]

ORR/OER polarization curves were tested to further investigate the electrocatalytic performance of Fe_2O_3 nanoflakes. Fig. 2b illustrates the linear sweep voltammograms from 3.0 to 2.0 V at 2 mV/s for ORR activities. The Super P electrode containing Fe_2O_3 nanoflakes shows the improved ORR activity compared to the pure Super P by demonstrating the value of the onset potential and limiting current of ORR for the electrode containing Fe_2O_3 nanoflakes higher than the pure Super P electrode. Furthermore, it can be observed that the electrode containing Fe_2O_3 exhibits a superior ORR kinetics, which

[z]E-mail: zza75@163.com; laiyanqingcsu@163.com

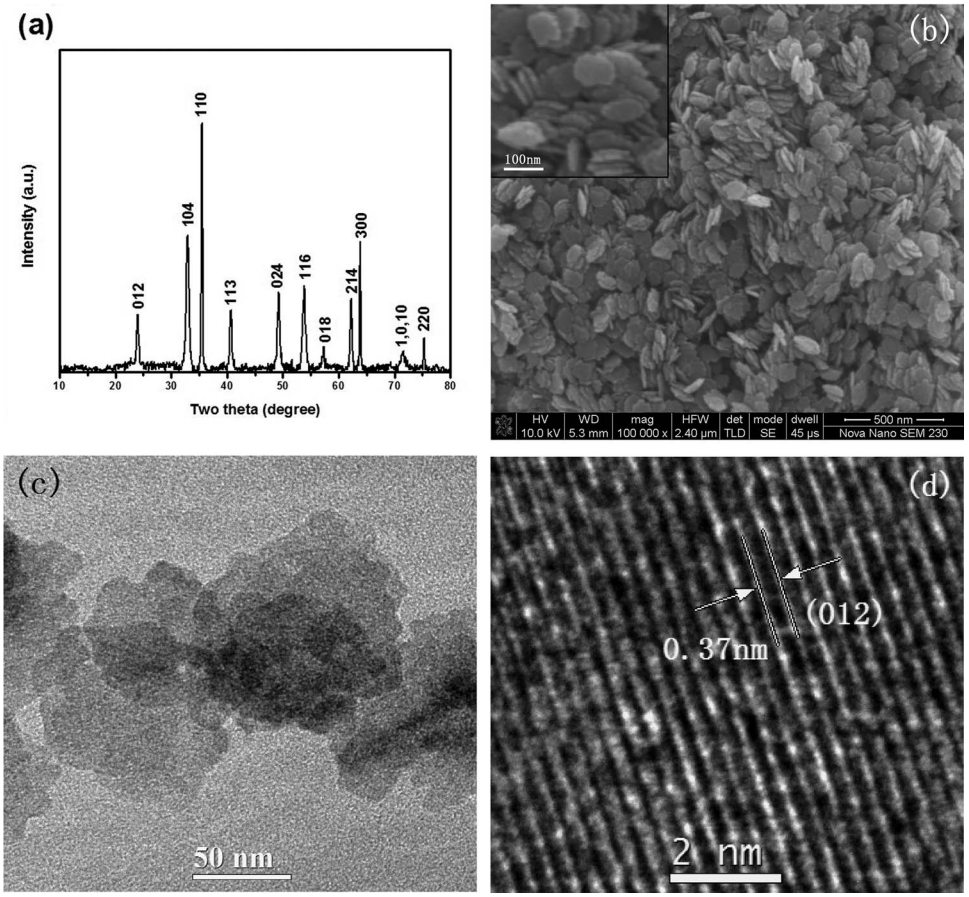

Figure 1. (a) XRD pattern, (b) SEM image, (c) TEM and (d) HRTEM image of the Fe_2O_3 nanoflakes.

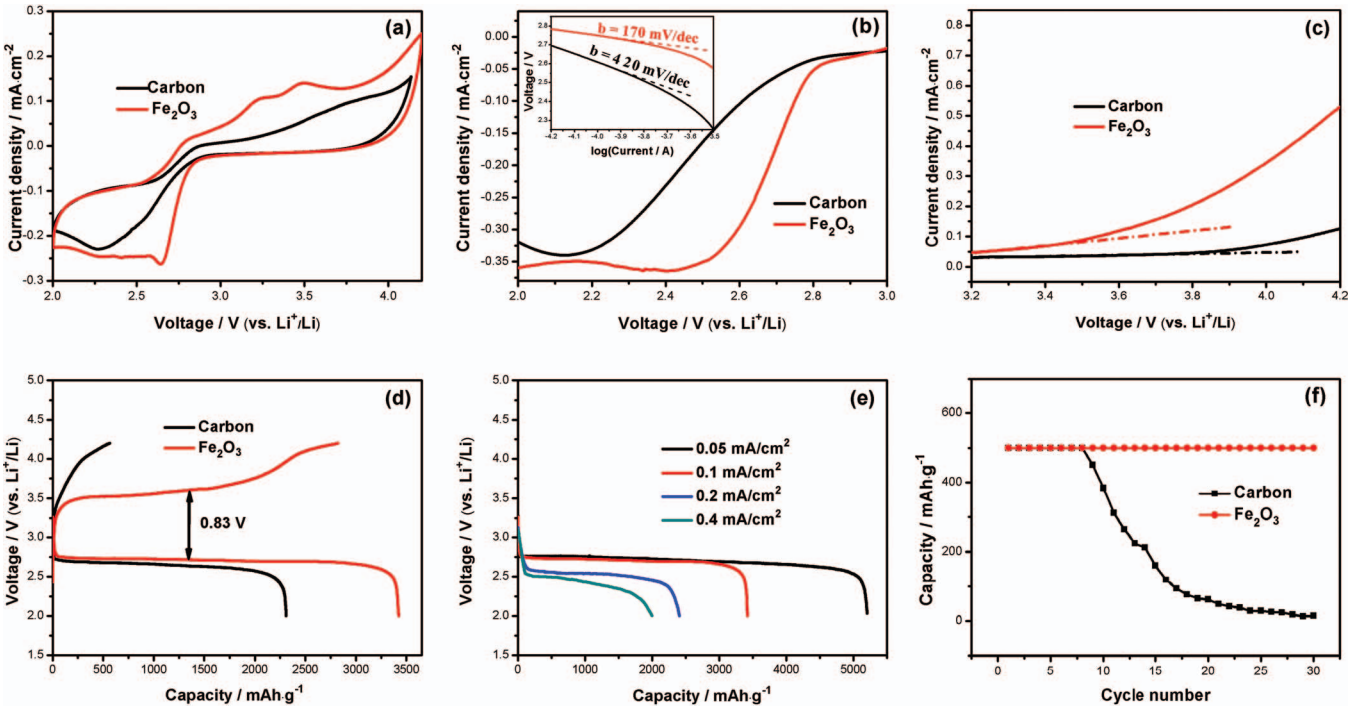

Figure 2. (a) CV curves at a scan rate of 0.5 mV/s; (b) linear sweep voltammetry curves and Tafel plots (inset) of ORR, and (c) linear sweep voltammograms of OER at a scan rate of 2 mV/s; (d) discharge/charge curves at a current density of 0.1 mA/cm^2; (e) discharge behavior of Fe_2O_3 nanoflakes in various current densities; (f) cycle performance with a restriction of the capacity to 500 mAh/g at a current density of 0.1 mA/cm^2.

was evidenced by a smaller Tafel slope of 170 mV/decade than that of pure Super P (420 mV/decade) as showed by the insert in Fig. 2b. This result indicates the excellent catalytic performance for ORR of Fe_2O_3 nanoflakes.[7] The linear sweep voltammograms of the cells for OER were also evaluated as shown in Fig. 2c. The electrode containing Fe_2O_3 nanoflakes exhibits an obviously higher OER current and lower onset potential.[6] These results also suggest that Fe_2O_3 nanoflakes have high electrocatalytic activity for ORR and OER in non-aqueous Li-air batteries.

Fig. 2d shows that the discharge and charge curves of the two different electrodes, at a current density of 0.1 mA/cm^2. It is found that the electrode containing Fe_2O_3 nanoflakes exhibits a high discharge potential plateau at ∼2.75 V vs. Li^+/Li and a specific capacity of ∼3420 mAh/$g_{electrode}$ calculated based on the total weight of electrode (∼4560 mAh/g_{carbon} based on carbon), which is about 49% higher than that of pure Super P electrode (∼2300 mAh/$g_{electrode}$, with a potential plateau at ∼2.68 V vs. Li^+/Li). Meanwhile, there is a low charge voltage for the electrode containing Fe_2O_3 nanoflakes at ∼3.58 V, corresponding with a narrow voltage gap of ∼0.83 V, which is as low as PtAu,[14] and is more excellent than many reported catalysts such as α-MnO_2,[5] Co_3O_4,[11] Fe_2O_3/graphene etc.[12] This result is consistent with CVs and polarization curves.

Fig. 2e shows the discharge profiles of the electrode containing Fe_2O_3 nanoflakes at various current densities. It can be seen that the discharge capacity and potential plateau decrease with increasing current density, which is consistent with previous reports that oxygen diffusion becomes the main constraints at a higher current density.[4,11] The Li–air battery shows the very high capacity of about ∼5200 mAh/$g_{electrode}$ at a current density of 0.05 mA/cm^2, and an appreciable capacity of ∼2000 mAh/$g_{electrode}$ is retained even at a high current density of 0.4 mA/cm^2.

In order to further investigate with the cycle performance of the electrode containing Fe_2O_3 nanoflakes for Li-air battery, the current electrochemical measurement protocol by limiting the depth of the discharge was employed.[19] Fig. 2f reveals the cycle performance of the electrode containing Fe_2O_3 and the pure Super P electrode by controlling discharge depth to 500 mAh/$g_{electrode}$ at the current density of 0.1 mA/cm^2. Li-air cells with the electrode containing Fe_2O_3 nanoflakes can maintain the cycle stability for over 30 cycles. As a comparison, the cells with the pure Super P electrode can only last for 8 cycles. The superior performance of the electrode containing Fe_2O_3 nanoflakes may be attributed to the efficient electrocatalytic activities of iron oxide-based catalysts toward O_2 and their nanoscale size for increasing active sites.[11,12] These facts clearly indicate the feasibility of Fe_2O_3 as a catalyst for Li-air battery, and should be further investigated.

Conclusions

In summary, Fe_2O_3 nanoflakes with the average diameter of ∼90 nm were prepared by a simple hydrothermal method. And this Fe_2O_3 nanoflakes exhibit superior catalytic properties for both ORR and OER processes in Li–air batteries with a low voltage gap of ∼0.83 V. The batteries also exhibit considerable rate capability and cyclic ability. This study suggests that nanoflake-structured Fe_2O_3 have the potential to be alternative catalyst for Li-air batteries.

References

1. K. M. Abraham and Z. Jiang, *J. Electrochem. Soc.*, **143**(1), 1 (1996).
2. G. Girishkumar, B. McCloskey, A. C. Luntz, S. Swanson, and W. Wilcke, *J. Phys. Chem. Lett.*, **1**(14), 2193 (2010).
3. T. Ogasawara, A. Débart, M. Holzapfel, P. Novak, and P. G. Bruce, *J. Am. Chem. Soc.*, **128**(4), 1390 (2006).
4. J. Li, B. Peng, G. Zhou, Z. Zhang, Y. Lai, and M. Jia, *ECS Electrochem. Lett.*, **2**(2), A25 (2013).
5. A. Débart, A. J. Paterson, J. Bao, and P. G. Bruce, *Angew. Chem. Int. Ed.*, **120**(24), 4597 (2008).
6. F. Li, R. Ohnishi, Y. Yamada, J. Kubota, K. Domen, A. Yamada, and H. Zhou, *Chem. Commun.*, **49**(12), 1175 (2013).
7. Y. C. Lu, H. A. Gasteiger, and S. H. Yang, *Electrochem and Solid-State Lett.*, **14**(5), A70 (2011).
8. R. Padbury and X. Zhang, *J. Power Sources*, **196**(10), 4436 (2011).
9. F. Li, T. Zhang, and H. Zhou, *Energy Environ. Sci.*, **6**(4), 1125 (2013).
10. K. Zhang, L. Zhang, X. Chen, X. He, X. Wang, S. Dong, P. Han, C. Zhang, S. Wang, L. Gu, and G. Cui, *J. Phys. Chem. C*, **117**(2), 858 (2013).
11. Y. Cui, Z. Wen, and Y. Liu, *Energy Environ. Sci.*, **4**(11), 4727 (2011).
12. W. Zhang, Y. Zeng, C. Xu, H. Tan, W. Liu, J. Zhu, N. Xiao, H. H. Hng, J. Ma, H. E. Hoster, R. Yazami, and R. Yan, *RSC Advances*, **2**(22), 8508 (2012).
13. R. S. Kalubarme, C. H. Ahn, and C. J. Park, *Scripta Materialia*, **68**(8), 619 (2013).
14. Y. C. Lu, Z. Xu, H. A. Gasteiger, S. Chen, K. Hamad-Schifferli, and Y. Shao-Horn, *J. Am. Chem. Soc.*, **132**(35), 12170 (2010).
15. X. Ren, S. S. Zhang, D. T. Tran, and J. Read, *J. Mater. Chem.*, **21**(27), 10118 (2011).
16. M. Lefevre, E. Proietti, F. Jaouen, and J. P. Dodelet, *Science*, **324**(5923), 71 (2009).
17. X. Li, Y. Lei, X. Li, S. Song, C. Wang, and H. Zhang, *Solid State Sciences*, **13**(12), 2129 (2011).
18. C. O. Laoire, S. Mukerjee, and K. M. Abraham, *J. Phys. Chem. C*, **114**(19), 9178 (2010).
19. D. Xu, Z. Wang, J. Xu, L. Zhang, and X. Zhang, *Chem. Commun.*, **48**(55), 6948 (2012).